

BIROn - Birkbeck Institutional Research Online

Troker, Martina and Waksman, Gabriel (2018) Translocation through the conjugative Type 4 secretion system requires unfolding of its protein substrate. *Journal of Bacteriology* 200 (6), JB.00615-17. ISSN 0021-9193.

Downloaded from: <https://eprints.bbk.ac.uk/id/eprint/21104/>

Usage Guidelines:

Please refer to usage guidelines at <https://eprints.bbk.ac.uk/policies.html>
contact lib-eprints@bbk.ac.uk.

or alternatively

Martina Trokter¹ and Gabriel Waksman^{1,*}

¹Institute of Structural and Molecular Biology, Department of Biological Sciences,
Birkbeck, Malet Street, London WC1E 7HX, UK

*Author for correspondence: g.waksman@mail.cryst.bbk.ac.uk

Abstract

Bacterial conjugation, a mechanism of horizontal gene transfer, is the major means by which antibiotic resistance spreads among bacteria (1,2). Conjugative plasmids are transferred from one bacterium to another through a type IV secretion system (T4SS) in a form of single-stranded DNA covalently attached to a protein called relaxase. The relaxase is fully functional both in a donor cell (prior to conjugation) and recipient cell (after conjugation). Here we demonstrate that the protein substrate has to unfold for efficient translocation through the conjugative T4SS. Furthermore, we present various relaxase modifications that preserve the function of the relaxase but block substrate translocation. This study brings us a step closer to deciphering the complete mechanism of T4SS substrate translocation, vital for development of new therapies against multidrug-resistant pathogenic bacteria.

Importance

Conjugation is the principal means by which antibiotic resistance genes spread from one bacterium to another (1,2). During conjugation, a covalent complex of single-stranded DNA and a protein termed relaxase is transported by a type IV secretion system. To date, it is not known whether the relaxase requires unfolding prior to transport. In this report, we use functional assays to monitor the transport of relaxase wild-type and variants containing unfolding-resistant domains and show that these domains reduce conjugation and protein transport dramatically. Mutations that lower the free energy of unfolding in these domains do not block translocation and can even promote it. We thus conclude that the unfolding of the protein substrate is required during transport.

Introduction

Bacteria have evolved a diversity of specialized secretion systems that allows them to translocate macromolecules across the cell envelope (3). Among them, the type IV secretion system (T4SS) is the most versatile (4). T4SSs mediate the transfer of DNA and protein substrates across the cell envelopes. The largest and most widely distributed of the T4SS subfamilies are conjugation systems (5).

Conjugation is a major mechanism of horizontal gene transfer (6,7). It is a process by which one bacterium, the donor, transfers genetic material to another bacterium, the recipient, in a contact-dependent manner (8). Thus, conjugation is the major means by which antibiotic resistance genes spread among bacterial populations (1,2). Conjugation is widely distributed among Gram-negative bacteria, Gram-positive bacteria, and even some archaea (9).

Many plasmids and integrative and conjugative elements (ICEs), so-called "mobile elements", undergo conjugation (10). Many of these mobile genetic elements are self-transmissible: they encode the entire machinery necessary for their transfer into recipient cells. Proteins necessary for conjugation assemble into two complexes: a DNA-processing complex called the relaxosome and a complex responsible for transfer, the T4SS. The relaxosome is an assembly of a protein called relaxase and a few accessory proteins that bind a specific DNA sequence called *oriT* (origin of transfer) to form a nucleo-protein complex (11). The T4SS is a large (3-4 MegaDalton) protein complex consisting of a transport apparatus that spans the bacterial cell envelope (12), a pilus that extends from the cell surface (13) and mediates contact between cells (14), and a type IV coupling protein (T4CP) (15,16) that recruits the relaxosome to the secretion channel.

The general mechanism of conjugation is still poorly understood but some steps are known (11,17). The relaxase encoded by a number of plasmids (but not all) is an enzyme that often carries two activities, a transesterase/nicking activity and a helicase activity. The transesterase nicks the plasmid DNA strand destined for

67 transfer (T-strand) at a specific position within *oriT*, called *nic*, and remains covalently
 68 attached through a catalytic tyrosine to the 5' phosphate end of the cleaved strand.
 69 The relaxase and accessory proteins carry translocation signals for recruitment of the
 70 transfer intermediate to T4SS via T4CP. Upon contact with a recipient cell, the
 71 substrate - the relaxase covalently attached to the T-strand - is transported into the
 72 recipient cell in an ATPase-dependent manner. During the translocation process, the
 73 T-strand is unwound from its complementary strand by a second copy of the
 74 relaxase, the helicase activity of which motors the T-strand through the T4SS,
 75 presumably assisted by some of the T4SS ATPases (18). In the recipient cell, the
 76 relaxase molecule that has passed through the system may recircularize the T-
 77 strand, and the complementary strand is synthesized (17).

78 R388 is one of the best-studied conjugative plasmids that belong to a broad-
 79 host-range group of plasmids (19,20). Proteins essential for conjugation are encoded
 80 within two separate gene clusters. One cluster contains *oriT* and genes encoding the
 81 accessory protein TrwA, the T4CP protein TrwB, and the relaxase TrwC, whereas
 82 the other cluster encodes eleven T4SS proteins, TrwN-TrwD, homologs of the VirB1-
 83 VirB11 proteins of the prototypical T4SS from *Agrobacterium tumefaciens*, the
 84 VirB/D4 system (21,22).

85 The TrwC relaxase is a 107 kDa protein composed of two domains: an N-
 86 terminal transesterase (also termed "relaxase") domain (approx. 1-300 residues) and
 87 a C-terminal helicase domain (approx. 300-966 residues). High-resolution crystal
 88 structures of TrwC relaxase domain in complex with oligonucleotides containing
 89 TrwC binding and/or nicking sites revealed details of DNA binding site recognition
 90 and nicking mechanism by TrwC (23,24). Nucleophilic attack of the *nic* site by the
 91 catalytic tyrosine, Tyr18 (25), generates a phosphotyrosine bond between the
 92 cleaved T-strand 5' phosphate and the Tyr residue in the relaxase. The C-terminus of
 93 TrwC (residues 796-802) contains a translocation signal for recruitment by the T4SS
 94 machinery (26). The helicase domain contains a 5'-3' helicase activity (27). Once in

95 the recipient cell, the helicase domain is thought to track 5'–3' along the T-strand in
96 order to position it correctly for the termination rejoining step (28). It is also thought to
97 be responsible for the unwinding of the T-strand during conjugation. In this case, the
98 T-strand unwinding TrwC molecule would have to be distinct from the translocated
99 one (18).

100 The fact that the relaxase has to pass through the T4SS raises the question
101 whether the relaxase is transported in a folded or unfolded state through the T4SS
102 channel. Among other types of bacterial secretion systems, some are known to
103 transport folded substrates (such as type 2 secretion systems (29) and chaperone-
104 usher pathway (30,31)), whereas some can translocate only unfolded substrates
105 (e.g. type 1 secretion systems (32) and type 3 secretion systems (33,34)). The
106 negative stain-electron microscopy structure of the TrwM/VirB3-TrwE/VirB10
107 complex from R388 T4SS has recently revealed the T4SS architecture (12).
108 However, the internal channel, the dimensions of which might give a clue on the
109 folding state of the substrate during transport, has not been identified yet. In this
110 report, we have studied the requirements for the substrate translocation by the R388
111 conjugative T4SS. We show that the T4SS substrates have to be unfolded in order to
112 be translocated into recipient cells.

113

114 **Results**

115 The overall aim of this study is to investigate whether transport of the relaxase
116 requires unfolding of the protein. In order to answer this question, our strategy was
117 to fuse unfolding-resistant proteins or protein modules of various sizes to TrwC and
118 test if they can be transported into recipient cells. We first sought to test this by
119 directly monitoring the transport of the protein itself during conjugation using the
120 previously described Cre recombinase reporter assay for translocation (CRAFT
121 (35,36)).

122

123 Establishing a translocation assay of the TrwC relaxase based on the CRAFT assay

124 Briefly, the recipient strain contains a chloramphenicol resistance gene
 125 interrupted by a tetracyclin resistance cassette flanked by *loxP* sites. Therefore, the
 126 strain is tetracyclin resistant, but upon Cre recombination becomes tetracyclin
 127 sensitive and chloramphenicol resistant. The transfer of Cre recombinase-substrate
 128 fusion can be measured by measuring the change in antibiotic resistance of recipient
 129 cells upon conjugation. We used a two-plasmid system composed of a plasmid
 130 containing R388 *oriT*, termed pRSF-oriT, and a plasmid encoding relaxosome
 131 components (TrwA, TrwB, and TrwC) and T4SS, termed pBAD-ABC-T4SS. This two-
 132 plasmid system typically resulted in 60-80% recipients acquiring the *oriT* plasmid
 133 (transconjugants) in our conjugation assay.

134 We first fused the Cre recombinase at different locations within the TrwC
 135 substrate and tested which construct retains functionality (both in plasmid
 136 conjugation and Cre recombination). Cre recombinase was fused to the TrwC N-
 137 terminus (termed Cre-TrwC), TrwC C-terminus (termed TrwC-Cre) and in between
 138 the relaxase and helicase domains (termed R-Cre-H) (Fig. 1A). Given the fact that
 139 the first methionine (Met1) of the N-terminal relaxase domain is located at the center
 140 of the relaxase structure and participates in DNA binding, together with Leu2, His4,
 141 Met5, and Val6 (24), there was a possibility that the N-terminal fusion might abolish
 142 *oriT* binding and/or nicking, and therefore conjugation. Nevertheless, TrwC transfer
 143 without DNA transfer has previously been observed (37) and, thus, we proceeded
 144 with making and testing all three Cre fusions of TrwC, even the N-terminal one.

145 Cre recombinase retained functionality in all three fusions (Fig. 1B).
 146 Surprisingly, conjugation level of all three fusions was high, even for the N-terminal
 147 fusion; however, protein transfer was detected only in the case of Cre-TrwC and R-
 148 Cre-H (Fig. 1C). Since TrwC-Cre is not transported into the recipient cells at
 149 detectable levels, the high conjugation efficiency observed with this construct is most

150 likely due to a fraction of TrwC lacking the C-terminal Cre fusion - a result of
151 proteolytic degradation within the cell.

152 Cre-TrwC displays a high level of conjugation, indicating that N-terminal
153 fusions of TrwC might be active in DNA transport after all. We therefore tested
154 purified TrwC with and without N-terminal fusions in an *oriT* nicking assay. As shown
155 in Fig. 2, whereas TrwC-His₆ formed a covalent linkage with pUC-oriT plasmid, we
156 did not detect any mGFP-TrwC, or even GA-TrwC (TrwC with an additional N-
157 terminal glycine and alanine residue) covalently bound to *oriT*. Since even only two
158 additional N-terminal residues can abolish TrwC activity, the source of TrwC protein
159 that is functional in conjugation is most likely wild type TrwC co-expressed starting
160 from the original start codon. The linker sequence between Cre and TrwC that lies
161 just upstream of the TrwC start codon is rich in GG nucleotides, possibly acting as a
162 ribosome-binding site. In conclusion, both N-terminal and C-terminal fusions abolish
163 TrwC transport and/or activity.

164 Unlike the N-terminal and C-terminal Cre fusions, which can both apparently
165 yield a Cre-less, wild-type version of the protein (see above), the internal Cre fusion
166 construct cannot undergo modifications yielding wild-type TrwC. Indeed, separated
167 relaxase and helicase domains that could arise by proteolytic degradation are not
168 functional (27,38). Therefore, the measured conjugation efficiency of R-Cre-H
169 reflects the activity of the full-length protein. R-Cre-H also showed almost two orders
170 of magnitude higher level of protein translocation in the CRAfT experiment in
171 comparison to Cre-TrwC (Fig. 1C). Since Cre-TrwC is not functional in *oriT* nicking,
172 the protein is in this case transported without being attached to the T-strand as
173 described in Draper et al. 2005 (37). In order to test if *oriT* binding is the reason for
174 higher protein translocation of R-Cre-H, we repeated the CRAfT assay but this time
175 excluding the pRSF-oriT plasmid. Surprisingly, we detected higher protein transport
176 in the absence of *oriT* plasmid than in its presence (Fig. 1D). This indicates that the
177 Cre recombination in recipient cells might be affected by the presence of the T-

178 strand, possibly due to a competition with the TrwC helicase activity along the T-
179 strand.

180

181 Substrate unfolding is a pre-requirement for translocation through T4SS

182 Next, we chose the N-terminal fusions to test the extent of substrate unfolding
183 required for its transport through T4SS. We fused a set of unfoldable (this word is
184 used here to mean “that can be unfolded”) and unfolding-resistant (that cannot be
185 unfolded) proteins between Cre and TrwC (Fig. 3A) and tested if they can be
186 transported into recipient cells. With Cre recombinase positioned at the very N-
187 terminus and TrwC translocation signal at the very C-terminus, these constructs
188 allow us to detect the transport of only full-length proteins. Ubiquitin (Ub; 8 kDa) and
189 GFP (27 kDa) have been reported to be resistant to unfolding, whereas the ubiquitin
190 mutant Ub^{I3G,I13G} (Ub^{3,13}) served as the unfoldable protein control (34,39). We first
191 tested the Cre recombinase activity of these constructs. Cre recombinase was
192 functional in all fusions tested (Fig. 3B).

193 When tested in the CRAFT assay, the protein construct containing the
194 unfoldable fusion, the ubiquitin mutant (Ub^{3,13}), was transported into recipient cells at
195 very high levels (~10% recipient cells underwent recombination; Fig. 3C). In
196 comparison, its wild-type ubiquitin counterpart was transported at about five orders of
197 magnitude lower level, similar to the construct containing mGFP. These data clearly
198 demonstrate that the conjugative T4SS substrate, the relaxase protein, has to be
199 unfolded in order to pass through the T4SS channel.

200

201 Relaxase constructs that block substrate translocation in the native plasmid

202 Experiments above were conducted using an artificial two-plasmid system
203 reporting on protein transport to the recipient cell. We sought next to monitor the
204 nucleoprotein substrate transport through conjugative T4SS using the native R388
205 plasmid. We also sought to expand the range of fusion proteins probed. For this

206 purpose, it was necessary to generate a modified protein substrate that is fully
207 functional. We therefore generated three different sets of relaxase constructs and
208 tested their functionality. For these experiments, we directly modified TrwC in the
209 wild-type R388 plasmid. Since N-terminal fusions abolish *oriT* nicking activity, we
210 tested if duplicating the relaxase domain in front of the N-terminal fusion can recover
211 relaxase activity (Fig. 4A left). In order to avoid expression of the wild-type TrwC from
212 its original start codon, the first methionine in the second relaxase domain was
213 deleted. Indeed, the addition of the relaxase domain in front of the unfoldable
214 ubiquitin fusion resulted in wild-type levels of relaxase activity (Fig. 4A right). The
215 high conjugation efficiency of this construct is not the result of proteolysis of mutant
216 ubiquitin (Fig. S1). Replacing an unfoldable fusion with an unfolding-resistant one
217 efficiently blocks the substrate transport, resulting in more than two orders of
218 magnitude lower conjugation efficiency (Fig. 4A right).

219 Equivalently, an attempt was made to recover the activity of C-terminal
220 fusions by adding another helicase domain (H) to the C-terminus of a TrwC-fusion
221 (Fig. 4B left). In this case, the duplication of the helicase domain did not completely
222 restore the wild-type level of relaxase activity (Fig. 4B right), potentially due to the
223 suboptimal position of the translocation signal (e.g. too large a distance between the
224 relaxase and the functional translocation signal). The difference in the conjugation
225 efficiency between the unfolding-resistant and unfoldable ubiquitin construct is lower
226 than for the constructs with the duplicated relaxase. The observed conjugation
227 efficiency of TrwC-Ub/mGFP-H constructs might be a result of either co-expression
228 of the wild-type TrwC (as a result of either degradation and/or premature translation
229 termination) or suboptimal folding of ubiquitin and mGFP at the TrwC C-terminus.

230 Finally, we tested the activity of TrwC containing internal fusions between its
231 relaxase and helicase domain (Fig. 4C left). Internal fusion with Ub^{3,13} retains wild-
232 type level of activity (Fig. 4C right). Unfolding-resistant (Ub or mGFP) fusions

233 efficiently blocked substrate transport, with conjugation efficiencies of more than
234 three orders of magnitude lower than its unfoldable counterpart.

235 We note that in all unfolding-resistant variants tested, a very low residual level
236 of translocation/transfer is observed, likely due to a small fraction of these proteins
237 being less resistant to unfolding, due to defects in their folded state.

238

239 **Conclusion**

240 Secretion in bacteria is a critical process in pathogenesis and inter-bacterial
241 competition in many bacterial pathogens. Bacteria have evolved a diversity of
242 specialized secretion systems to export a wide range of substrates, including small
243 molecules, proteins and DNA, across the cell envelope (3). Some secretion systems,
244 such as T2SS (29) and chaperone-usher pathway (30,31), transport fully folded
245 protein substrates, whereas some can transport only unfolded substrates (e.g. T1SS
246 (32) and T3SS (33,34)). In this report we demonstrate that conjugative T4SS
247 substrates, relaxases, have to undergo unfolding in order to be transported through
248 the T4SS channel. Comparison of translocation frequencies of unfolding-resistant
249 TrwC fusions and their unfoldable counterparts clearly demonstrated that both TrwC
250 alone and TrwC covalently attached to the T-strand are transported into recipient
251 cells in an unfolded state. In that respect, conjugative T4SSs works in a similar
252 manner as effector only-transporting T4SSs such as that of the bacterial pathogen
253 *Legionella pneumophila* (46).

254 T1SS substrates fold upon binding of calcium, which is low in the bacterial
255 cytosol, but high in the extracellular space, therefore it is generally assumed that
256 T1SS substrates adopt their folded conformation only after secretion into the
257 extracellular space. Conjugative relaxases are clearly folded prior to their
258 translocation, as they are fully functional when expressed in a bacterial cell. Which
259 enzyme/unfoldase is responsible for T4SS substrate unfolding remains unclear. In
260 case of T3SS, a dedicated hexameric ATPase has a critical function in substrate

261 recognition and unfolding in an ATP-dependent manner (33). T4SS, on the other
262 hand, is energized by three distinct hexameric ATPases: VirB4, VirB11 and T4CP.
263 T4CP is an integral membrane protein that interacts with the relaxase and accessory
264 proteins and recruits the transfer intermediate to the T4SS translocation machinery.
265 T4CP ATPase activity is not required for the recruitment (41). However, ATPase
266 activity of all three ATPases is essential for nucleoprotein transport (41). VirB4 is an
267 integral part of the T4SS inner-membrane complex (IMC) and is located mainly in the
268 cytoplasm. VirB11 is a cytoplasmic ATPase that interacts with T4CP and VirB4.
269 Apart from being essential for substrate transport, VirB4 and VirB11 are required for
270 T4SS pilus assembly. Due to their several roles that are essential for the T4SS
271 function, it is difficult to predict which ATPase is responsible for substrate unfolding.

272 The CRAFT experiments performed here also revealed that an N-terminal
273 fusion might abolish a relaxase function (Fig. 1). TrwC *oriT* nicking activity was
274 sensitive to addition of only two amino acids at its N-terminus (Fig. 2). The crystal
275 structure of TrwC relaxase domain in complex with its cognate DNA at *oriT* showed
276 that first five TrwC residues participate in binding DNA (24). The N-terminal
277 methionine alone forms multiple interactions with DNA. Its side chain is trapped in a
278 hydrophobic cage formed by a sharp U-turn of the T-strand DNA, whereas its amino
279 group forms a hydrogen bond with the DNA. Therefore, addition of any amino acids
280 to the relaxase N-terminus might perturb the *oriT* binding and result in an inactive
281 protein.

282 Finally, we showed here that although the terminal fusions abolish the
283 relaxase activity, it is possible to modify the relaxase in different ways in order to
284 preserve the functionality of its domains. Placing a fusion internally or duplicating a
285 domain can recover a relaxase activity, and unfolding-resistant fusions can be used
286 to efficiently block the substrate transport. This will be particularly important for
287 deciphering the complete mechanism of T4SS substrate translocation. T4SS
288 substrates modified with unfolding-resistant fusions at appropriate locations could be

289 used as a tool to efficiently trap the substrate during translocation. Structural studies
290 of the T4SS in complex with the substrate trapped within will allow defining the
291 substrate translocation path and T4SS conformational changes necessary for
292 translocation. Deciphering the details of T4SS translocation mechanism will be vital
293 to facilitate development of new therapies against multidrug-resistant pathogenic
294 bacteria.

295

296 **Methods**

297 Molecular biology

298 *oriT* and expression plasmids used in this study are described in Table S1.
299 Primer sequences are shown in Table S2. DNA fragments used for cloning were
300 amplified using Phusion High-Fidelity DNA Polymerase (NEB) following
301 manufacturer's instructions. Restriction enzymes were obtained from NEB. Unless
302 otherwise stated, antibiotic concentrations used were: kanamycin (Km) 30 µg/ml,
303 ampicillin (Amp) 100 µg/ml, tetracycline (Tc) 10 µg/ml, chloramphenicol (Cm) 10
304 µg/ml, streptomycin (Sm) 25 µg/ml, and trimethoprim (Tmp) 10 µg/ml.

305 pRSF-oriT was generated by ligation (Rapid DNA ligation Kit, Roche) of
306 amplified *oriT* and pRSFDuet-1 vector digested with *Bss*HI restriction enzyme. pUC-
307 oriT was generated by ligation of amplified *oriT* and pUC18 vector digested with
308 *Hind*III-HF and *Sac*I-HF restriction enzymes.

309 Unless otherwise stated, all plasmids used in this study were generated by
310 seamless cloning using In-Fusion HD Cloning Kit (Clontech). In most cases, the
311 constructs were generated by fusing two PCR fragments. In some cases (described
312 below), the constructs were generated by fusing a PCR fragment and a linearized
313 vector. pBAD-trwN/virB1-trwE/virB10_{Strep}-trwD/virB11 was cloned by amplifying
314 *trwD/virB11* and inserting it into pBAD-trwN/virB1-trwE/virB10_{Strep} plasmid (12) which
315 was linearized using *Bst*BI restriction enzyme. pBAD-ABC-T4SS was cloned by
316 amplifying *trwABC_{HIS}* and inserting it into pBAD-trwN/virB1-trwE/virB10_{Strep}-

317 trwD/virB11 plasmid which was linearized using *Nco*I restriction enzyme. All pBAD-
318 ABC-T4SS constructs encoding modified TrwC were cloned in the same way (by
319 amplifying ABC and inserting into linearized pBAD-trwN/virB1-trwE/virB10^{Strep}-
320 trwD/virB11 plasmid).

321 TrwC internal fusions were inserted into an unstructured region between the
322 relaxase and helicase domains (between residue 312 and 313). The TrwC secondary
323 structure was predicted using PSIPRED v3.3 (<http://bioinf.cs.ucl.ac.uk/psipred/>).

324 Ubiquitin mutant was generated using QuikChange Lightning Multi Site-
325 Directed Mutagenesis Kit (Agilent Technologies) following manufacturer's
326 instructions. Cre active site mutant was generated using QuikChange Lightning Site-
327 Directed Mutagenesis Kit (Agilent Technologies) following manufacturer's
328 instructions.

329

330 Modification of the wild-type R388 plasmid

331 Modified R388 plasmids used in this study are described in table S3. The
332 R388 plasmid was modified using recombineering method following the multicopy
333 plasmid modification protocol (42,43). The two-step seamless method using the *cm*-
334 *sacB* selection cassette was used to create precise genetic changes without
335 otherwise altering the plasmid. The *cm-sacB* cassette is used for positive/negative
336 selection; it can be selected either for (by chloramphenicol resistance) or against
337 (sucrose sensitivity). In the first recombineering step, the sequence to be modified is
338 replaced with the *cm-sacB* cassette; the cassette is then replaced with the desired
339 alteration in the second recombineering event.

340 The bacterial strain containing the defective λ prophage, SW102 (44), and the
341 plasmid containing *cm-sacB* cassette, pEL04, were obtained from NCI-Frederick.
342 PCR products used for homologous recombination contained at each end on
343 average about 200 base pairs of flanking homology to the desired region on the
344 plasmid. For this purpose, PCR templates were first generated using In-Fusion HD

345 Cloning Kit. We first made the templates for the second recombineering step by
346 modifying TrwC encoded on the pBAD-ABC vector (see tables S1 and S2). The
347 templates for the first recombineering step were then prepared by replacing a desired
348 TrwC modification on a relevant pBAD-ABC vector (encoding relevant modified
349 TrwC) with the *cm-sacB* cassette. PCR products were amplified from linearized
350 templates using Phusion High-Fidelity DNA Polymerase (NEB), digested with *DpnI*,
351 and purified using MinElute Gel Extraction Kit (Qiagen). The details of the templates
352 and PCR products are given below.

353 To generate R388 plasmid encoding TrwC with a fusion protein in between
354 the relaxase (R) and helicase domains (H), R388_R-Ub/Ub^{3,13}/mGFP-H, the template
355 for the first recombineering step was generated by replacing the relaxase and the
356 first part of helicase domain in pBAD-ABC_{His} plasmid with *cm-sacB* cassette,
357 generating pBAD-AB_Cm-SacB-H plasmid. In the first recombineering step, the PCR
358 fragment containing B_Cm-SacB-H was amplified from pBAD-AB_Cm-SacB-H
359 plasmid and used to modify the wild-type R388. In the second recombineering step,
360 the PCR fragment containing B_R-Ub/Ub^{3,13}/mGFP-H was amplified from pBAD-
361 AB_R-Ub/Ub^{3,13}/mGFP-H plasmid and used to modify R388_B_Cm-SacB-H.

362 To generate wild-type R388 plasmid encoding TrwC with duplicated domains,
363 four recombineering steps were necessary. The two-step approach, using a PCR
364 product with duplicated domain sequences in the second step, generated R388
365 plasmid encoding wild-type TrwC. This is because the recombineering occurs
366 through a fully ssDNA intermediate of the PCR fragment (45), most likely resulting in
367 recombination of the duplicated domains, generating the wild-type protein.

368 To generate R388 plasmid encoding TrwC with duplicated relaxase domains
369 (R) and a fusion protein in between, R388_R-Ub/Ub^{3,13}/mGFP-TrwC, following PCR
370 fragments were generated. For the first recombineering step, the PCR fragment
371 encoding B_Cm-SacB-H was amplified from pBAD-AB_Cm-SacB-H plasmid. For the
372 second step, the PCR fragment encoding B_R-His₆-Ub/Ub^{3,13}/mGFP-H was amplified

373 from pBAD-AB_R-His₆-Ub/Ub^{3,13}/mGFP-H plasmid. For the third step, the PCR
374 fragment encoding Ub/Ub^{3,13}/mGFP-Cm-SacB-H was amplified from pBAD-AB_R-
375 His₆-Ub/Ub^{3,13}/mGFP-Cm-SacB-H plasmid. For the fourth step, the PCR fragment
376 encoding Ub/Ub^{3,13}/mGFP-TrwC was amplified from pBAD-AB_R-His₆-
377 Ub/Ub^{3,13}/mGFP-TrwC plasmid.

378 To generate R388 plasmid encoding TrwC with duplicated helicase domains
379 (H) and a fusion protein in between, R388_TrwC-Ub/Ub^{3,13}/mGFP-H, following PCR
380 fragments were generated. For the first step, the PCR fragment encoding H-Cm-
381 SacB-B11 was amplified from pBAD-ABC-Cam-SacB-trwD/virB11 plasmid.
382 TrwD/VirB11 is the protein encoded downstream of TrwC in the wild-type R388
383 plasmid. For the second step, the PCR fragment encoding H-Ub/Ub^{3,13}/mGFP-His₆-
384 B11 was amplified from pBAD-ABC-Ub/Ub^{3,13}/mGFP-His₆-trwD/virB11 plasmid. For
385 the third step, the PCR fragment encoding Ub/Ub^{3,13}/mGFP-Cm-SacB-trwD/virB11
386 was amplified from pBAD-ABC-Ub/Ub^{3,13}/mGFP-Cm-SacB-trwD/virB11 plasmid. For
387 the fourth step, the PCR fragment encoding Ub/Ub^{3,13}/mGFP-H-His₆-trwD/virB11 was
388 amplified from pBAD-AB_R-Ub/Ub^{3,13}/mGFP-H-His₆-trwD/virB11 plasmid.

389 Electrocompetent SW102 cells were prepared in the following way. 1.5 ml of
390 SW102 cells grown overnight at 30°C were diluted in 75 ml LB medium and grown
391 shaking at 32°C until reaching OD₆₀₀ of 0.5. The λ recombination genes were
392 induced by placing the flask into a 42°C shaking water bath for 15 min. The flask was
393 then cooled in the ice-water slurry and the electrocompetent cells were prepared by
394 washing the cells twice with 40 ml ice-cold distilled water and resuspending in 200 μ l
395 distilled water. 50 μ l cells were electroporated with 60 ng plasmid and 100-150 ng
396 purified PCR fragment and shaken for 2 hours at 30°C in 1 ml LB. After 2h, 9 ml of
397 LB medium containing 12.5 μ g/ml chloramphenicol (in the case of first
398 recombineering step) or 10 μ g/ml trimethoprim (in the case of second
399 recombineering step) was added and the culture was grown overnight shaking at
400 30°C. The following morning, the plasmid was isolated from the culture using

Trocter and Waksman (2017)

401 QIAprep Spin Miniprep Kit (Qiagen), transformed into electrocompetent TOP10 cells,
402 and recombined plasmid was selected on LB agar plates containing chloramphenicol
403 (in the case of first recombineering step) or trimethoprim and 6% sucrose and lacking
404 NaCl (in the case of second recombineering step). Several Cm-resistant and
405 sucrose-sensitive colonies (in the case of first recombineering step) or Cm-sensitive
406 and sucrose- and Tmp-resistant colonies (in the case of second recombineering
407 step) were grown and recombinant plasmids isolated and sequenced.

408

409 Cre recombination test

410 Prior to the CRAFT experiments described below, Cre recombinase activity for each
411 Cre fusion construct was tested. CSH26Cm::LTL cells (Tc^R; Lang et al. 2010)
412 carrying pBAD-ABC (Amp^R) with or without modified TrwC (as indicated in Results)
413 were grown overnight in LB medium containing tetracycline, ampicillin, and 0.4%
414 glucose. 125 µl of the overnight culture were pelleted and resuspended in 5 ml LB
415 medium containing ampicillin. The culture was grown at 37°C until reaching OD₆₀₀ of
416 0.6. The cells were then put on ice. Recombinants were selected by plating serial
417 dilutions on LB agar plates containing chloramphenicol, and total cell counts were
418 determined as the sum of cells growing on tetracycline plates and cells growing on
419 chloramphenicol plates. There were no cells growing on tetracycline and
420 chloramphenicol plates. The recombination frequencies are calculated as
421 recombinants per total amount of cells.

422

423 Cre recombinase reporter assay for translocation (CRAFT)

424 The Cre fusion reporter assay was adapted from Lang et al. 2010. An overnight
425 culture of TOP10 donor cells carrying pRSF-oriT (Km^R) and/or pBAD-ABC-T4SS
426 (Amp^R) with or without modified TrwC (as indicated in Results) was diluted 20x in LB
427 medium containing appropriate antibiotics and grown at 37°C until reaching OD₆₀₀ of
428 0.6. The cultures were then induced with 0.08% (vol/vol) arabinose for 1 hour. In

parallel, an overnight culture of CSH26Cm::LTL recipient cells (Tc^R) was diluted 40x in LB medium and grown at 37°C. Donors corresponding to OD of 1 and recipients corresponding to OD of 0.1 were spun and resuspended in 50 μ l LB. The mixture was pipetted onto a filter paper (MF-Millipore Membrane, mixed cellulose esters, 0.45 μ m) lying on top of an LB plate that was beforehand well dried. The filter was incubated at 37°C for 2.5 hours and then recovered into an Eppendorf tube. The cells were washed off the filter by adding LB medium and gently vortexing the tube. Recombinants were selected by plating serial dilutions on LB agar plates containing chloramphenicol, and when pRSF-oriT was present transconjugants were selected on LB agar plates containing kanamycin and tetracycline. Recipient cell counts were determined as the sum of cells growing on tetracycline plates and cells growing on chloramphenicol plates. No cells grew on tetracycline and chloramphenicol plates. The conjugation and protein translocation frequencies are calculated as transconjugants or recombinants per recipient respectively.

443

444 TrwC purification

445 A culture of *E. coli* TOP10 cells carrying pBAD-ABC_{His} (Amp^R) was grown at
446 37°C from a single colony until reaching OD₆₀₀ of 0.6. Protein expression was
447 induced with 0.08% (vol/vol) arabinose, and the culture was incubated overnight at
448 18°C shaking at 200 rpm. Cells were harvested and resuspended in ice-cold
449 resuspension buffer [50 mM HEPES, 15 mM imidazole, pH 7.8 at 4°C] supplemented
450 with 0.5 mg/ml lysozyme and protease inhibitors (Complete EDTA-free; Roche). After
451 resuspension, the lysate was supplemented with 5 mM $MgCl_2$ and 25 U/ml
452 benzonase (Merck Millipore) and incubated for 15 min on ice. The lysate was then
453 supplemented with 250 mM NaCl and passed through a high-pressure homogenizer
454 (Emulsiflex-C5; Avestin). The cell lysate was clarified by centrifugation at 100,000 g
455 for 30 min at 4 °C and applied to a 5-mL HiTrap Chelating HP column (GE
456 Healthcare) loaded with cobalt ions and equilibrated with wash buffer [50 mM

457 HEPES, 250 mM NaCl, 20 mM imidazole, pH 7.8 at 4°C]. The column was then
458 washed extensively first with wash buffer followed by high-salt buffer A [50 mM
459 HEPES, 500 mM NaCl, pH 7.8 at 4°C] and finally re-equilibrated with wash buffer.
460 The protein was eluted with 10 column volumes of linear imidazole gradient [A: wash
461 buffer; B: 50 mM HEPES, 200 mM NaCl, 500 mM imidazole, pH 8.0 at 4°C]. The
462 eluted protein was applied to a 5-mL HiTrap SP HP column (GE Healthcare)
463 equilibrated with low-salt buffer [50 mM HEPES, 250 mM NaCl, pH 7.8 at 4°C]. The
464 protein was eluted with 10 column volumes of linear salt gradient [A: low-salt buffer;
465 B: 50 mM HEPES, 1 M NaCl, pH 7.8 at 4°C]. The eluted protein was further purified
466 by gel filtration using a Superdex 200 10/300 GL column equilibrated in gel-filtration
467 buffer [50 mM HEPES, 500 mM NaCl, pH 7.8 at 4°C]. The protein concentration was
468 determined by measuring the absorbance at 280 nm and using a molar extinction
469 coefficient calculated from its primary sequence (Expasy;
470 <http://expasy.org/tools/protparam.html>). Proteins were supplemented with glycerol to
471 a final concentration of 20% (vol/vol), flash-frozen, and stored at -80°C.

472 mGFP-TrwC and GA-TrwC (TrwC with additional two residues, glycine and
473 alanine, at its N-terminus) were purified as described above for TrwC-His₆ with
474 following modifications. pETZt-mGFP-trwC and pETZt-trwC (Kn^R) were used to
475 transform *E. coli* BL21 Star (DE3) cells. Protein expression was induced with 0.1 mM
476 isopropylthio-β-galactoside (IPTG). In the case of GA-TrwC, following the ion-
477 exchange step, the N-terminal His₆-Z tag was cleaved off during an overnight
478 incubation at 4°C with His₆-tagged TEV protease (1 mg of protease per 30 mg of
479 substrate). The mixture was simultaneously dialyzed into wash buffer B [50 mM
480 HEPES, 500 mM NaCl, 20 mM imidazole, pH 7.8 at 4°C]. Cleaved His₆-Z tag and the
481 protease were removed by rebinding to a cobalt-charged HiTrap chelating HP
482 column equilibrated with wash buffer B. The flow-through (containing cleaved
483 proteins) was concentrated and further purified by gel filtration as described above.

484

485 *oriT* nicking assay

486 To test DNA nicking by different TrwC constructs, pUC-oriT was mixed with
 487 either TrwC-His₆, GA-TrwC, or mGFP-TrwC and incubated for 30 min at 37°C. The
 488 final mixture contained 40 nM pUC-oriT and 40, 80 or 160 nM TrwC, and the final
 489 binding buffer contained 30 mM HEPES pH 7.6 at 25°C, 100 mM NaCl, and 5 mM
 490 MgCl. After incubation, reaction mixtures were supplemented with NuPAGE LDS
 491 Sample Buffer (ThermoFisher Scientific) and EDTA at the final concentration of 1x
 492 and 5 mM, respectively. The samples were heated at 95°C for 5 min and loaded onto
 493 a NuPAGE Novex 4-12% Bis-Tris gel (ThermoFisher Scientific). Following SDS-
 494 PAGE, the gel was stained with SYPRORuby Protein Gel Stain (ThermoFisher
 495 Scientific) following manufacturer's instructions. TrwC constructs were visualized
 496 using a FLA-3000 fluorescent imaging scanner (FujiFilm).

497 To test its specificity of DNA nicking, TrwC-His₆ was mixed with either pUC-
 498 oriT or pUC18 plasmid and incubated for 30 min at 37°C. The final mixture contained
 499 50 or 100 nM TrwC-His₆ and 20 nM plasmid, and the final binding buffer contained
 500 30 mM HEPES pH 7.6 at 25°C, 100 mM NaCl, 5 mM MgCl₂, and 4% glycerol.
 501 After incubation, the samples were further processed as described above.

502

503 R388 conjugation assay

504 An overnight culture of TOP10 donor cells (Sm^R) carrying R388 plasmid (Tm^R) with
 505 wild-type or modified TrwC (as indicated in Results) was diluted 20x in LB medium
 506 and grown at 37°C until reaching OD of 0.6. In parallel, an overnight culture of
 507 CSH26Cm::LTL recipient cells (Tc^R) was diluted 30x in LB medium and grown at
 508 37°C. Donors corresponding to OD of 0.3 and recipients corresponding to OD of 0.6
 509 were spun and resuspended in 50 µl LB. This OD ratio corresponded to 3:1
 510 recipients per donor. The mixture was pipetted onto a filter paper as described for the
 511 CRAfT experiments and incubated at 37°C for 1.5 hours. The filter was then placed
 512 into an Eppendorf tube and cells were washed off by addition of LB medium and

gentle vortexing. Transconjugants were selected on LB agar plates containing tetracycline and trimethoprim. Donor cell counts were determined with streptomycin and trimethoprim, and recipient cell counts were determined with tetracycline. The conjugation frequencies are calculated as transconjugants per donor.

Data availability

All relevant data are available from the authors upon request.

Figure legends

Figure 1. Establishing Cre recombinase reporter assay for translocation of R388 T4SS substrates.

(A) Scheme of TrwC constructs with Cre recombinase fusion at different positions.

(B) Recombination efficiency of Cre recombinase fused to the TrwC N-terminus (Cre-TrwC), TrwC C-terminus (TrwC-Cre) and in between the relaxase and helicase domains (R-Cre-H) when expressed in recipient cells. Values represent the mean \pm SEM of four experiments. Unpaired t-test showed no significant difference between recombination efficiencies of Cre-TrwC, R-Cre-H, and TrwC-Cre ($P > 0.05$).

(C) Conjugation and protein translocation efficiency of cells carrying pRSF-oriT and pBAD-ABC-T4SS plasmid encoding modified TrwC as indicated. The efficiencies are expressed as a fraction of recipient cells that acquired pRSF-oriT plasmid (transconjugants) and TrwC fusion protein (recombinants), respectively. Values represent the mean \pm SEM of three experiments. Statistically significant differences (unpaired t test) between wild-type and Cre fusion construct conjugation frequencies are indicated. *, $P \leq 0.05$; **, $P \leq 0.01$; ***, $P \leq 0.001$.

(D) The comparison of TrwC translocation in the presence (red bars) or absence (grey bars) of pRSF-oriT plasmid. The protein translocation efficiencies are expressed as a fraction of recipient cells that acquired indicated TrwC fusion protein.

541 Values represent the mean \pm SEM of four experiments. Statistically significant
542 differences (unpaired t test) between translocation frequencies in the presence or
543 absence of *oriT* are indicated. *, $P \leq 0.05$; **, $P \leq 0.01$; ***, $P \leq 0.001$.

544

545 **Figure 2.** N-terminal fusions abolish TrwC nicking of *oriT*.

546 (A) SYPRORuby-stained SDS gel showing purified TrwC-His₆, GA-TrwC (glycine-
547 alanine-TrwC), and mGFP-TrwC free or covalently bound to pUC-*oriT*. 40, 80, or 160
548 nM TrwC constructs were incubated at 37°C for 30 min with 40 nM pUC-*oriT* before
549 the nicking reaction was stopped by adding SDS sample buffer and EDTA and
550 heating at 95°C.

551 (B) TrwC-His₆ nicks *oriT* specifically. 50 nM (lane 1,3) or 100 nM (lane 2,4) TrwC-His₆
552 was incubated with either pUC-*oriT* or pUC18 plasmid (20 nM) as indicated at 37°C
553 for 30 min before the reaction was stopped by adding SDS sample buffer and EDTA
554 and heating at 95°C.

555

556 **Figure 3.** TrwC unfolding is necessary for its translocation through T4SS.

557 (A) Scheme of TrwC constructs with N-terminal Cre recombinase followed by an
558 unfoldable (Ub^{3,13}) or unfolding-resistant (Ub, mGFP) fusion.

559 (B) Recombination efficiency of Cre recombinase fused to the N-terminus of the
560 indicated protein followed by TrwC when expressed in recipient cells. Values
561 represent the mean \pm SEM of three experiments. Statistically significant differences
562 (unpaired t test) between recombination efficiencies of Cre-TrwC and constructs with
563 an additional fusion are indicated. *, $P \leq 0.05$; **, $P \leq 0.01$; ***, $P \leq 0.001$.

564 (C) Protein translocation efficiency of cells carrying pBAD-ABC-T4SS plasmid
565 encoding modified TrwC as indicated. Values represent the mean \pm SEM of four
566 experiments. Statistically significant differences (unpaired t test) between protein

translocation efficiencies of Cre-TrwC and constructs with an additional fusion are indicated. *, $P \leq 0.05$; **, $P \leq 0.01$; ***, $P \leq 0.001$.

Figure 4. Conjugation of TrwC fusions in native R388 plasmid.

(A) Duplicated relaxase domain recovers *oriT* nicking activity of TrwC with N-terminal fusion. (Left) Scheme of TrwC constructs with duplicated relaxase domain and indicated fusion protein (termed R-X-TrwC, where X represents Ub^{3,13}, Ub, or mGFP). (Right) Conjugation efficiency of cells carrying R388 plasmid encoding modified TrwC as indicated. Values represent the mean \pm SEM of three experiments. Statistically significant differences (unpaired t test) between wild-type and fusion construct conjugation frequencies are indicated. *, $P \leq 0.05$; **, $P \leq 0.01$; ***, $P \leq 0.001$.

(B) Conjugation efficiency of TrwC-fusion-helicase constructs. (Left) Scheme of TrwC constructs with indicated fusion protein and duplicated helicase domain (termed TrwC-X-H, where X represents Ub^{3,13}, Ub, or mGFP). (Right) Conjugation efficiency of cells carrying R388 plasmid encoding modified TrwC as indicated. Values represent the mean \pm SEM of three experiments. Statistically significant differences (unpaired t test) between conjugation frequencies of indicated pairs of constructs are shown. *, $P \leq 0.05$; **, $P \leq 0.01$; ***, $P \leq 0.001$.

(C) TrwC relaxase and helicase domains retain their functionality after being separated by an internal fusion. (Left) Scheme of TrwC constructs with indicated internal fusion (termed R-X-H, where X represents Ub^{3,13}, Ub, or mGFP). (Right) Conjugation efficiency of cells carrying R388 plasmid encoding modified TrwC as indicated. Values represent the mean \pm SEM of three experiments. Statistically significant differences (unpaired t test) between wild-type and fusion construct conjugation frequencies are indicated. *, $P \leq 0.05$; **, $P \leq 0.01$; ***, $P \leq 0.001$.

595

596

597 **Acknowledgements**

598 We would like to thank Dr. Ellen L. Zechner for the CSH26Cm::LTL strain.

599

600 **Author contributions**601 MT and GW designed the experiments; MT performed the experiments; MT and GW
602 wrote the manuscript.

603

604 **Competing Financial Interests**

605 The authors declare they have no competing financial interests.

606

607 **References**

- 608 1. Guiney, D. G., Jr. (1984) Promiscuous transfer of drug resistance in gram-
609 negative bacteria. *J Infect Dis* **149**, 320-329
- 610 2. Mazel, D., and Davies, J. (1999) Antibiotic resistance in microbes. *Cell Mol*
611 *Life Sci* **56**, 742-754
- 612 3. Costa, T. R., Felisberto-Rodrigues, C., Meir, A., Prevost, M. S., Redzej, A.,
613 Trokter, M., and Waksman, G. (2015) Secretion systems in Gram-negative
614 bacteria: structural and mechanistic insights. *Nature reviews. Microbiology*
615 **13**, 343-359
- 616 4. Wallden, K., Rivera-Calzada, A., and Waksman, G. (2010) Type IV secretion
617 systems: versatility and diversity in function. *Cellular microbiology* **12**,
618 1203-1212
- 619 5. de la Cruz, F., Frost, L. S., Meyer, R. J., and Zechner, E. L. (2010)
620 Conjugative DNA metabolism in Gram-negative bacteria. *FEMS*
621 *microbiology reviews* **34**, 18-40
- 622 6. Arber, W. (2014) Horizontal Gene Transfer among Bacteria and Its Role in
623 Biological Evolution. *Life (Basel)* **4**, 217-224
- 624 7. Norman, A., Hansen, L. H., and Sorensen, S. J. (2009) Conjugative plasmids:
625 vessels of the communal gene pool. *Philos Trans R Soc Lond B Biol Sci* **364**,
626 2275-2289
- 627 8. Lederberg, J., and Tatum, E. L. (1953) Sex in bacteria; genetic studies,
628 1945-1952. *Science (New York, N.Y.)* **118**, 169-175
- 629 9. Alvarez-Martinez, C. E., and Christie, P. J. (2009) Biological diversity of
630 prokaryotic type IV secretion systems. *Microbiology and molecular biology*
631 *reviews : MMBR* **73**, 775-808

- 632 10. Johnson, C. M., and Grossman, A. D. (2015) Identification of host genes
633 that affect acquisition of an integrative and conjugative element in
634 *Bacillus subtilis*. *Molecular microbiology* **98**, 1222
- 635 11. Ilangovan, A., Connery, S., and Waksman, G. (2015) Structural biology of
636 the Gram-negative bacterial conjugation systems. *Trends in microbiology*
637 **23**, 301-310
- 638 12. Low, H. H., Gubellini, F., Rivera-Calzada, A., Braun, N., Connery, S.,
639 Dujeancourt, A., Lu, F., Redzej, A., Fronzes, R., Orlova, E. V., and Waksman,
640 G. (2014) Structure of a type IV secretion system. *Nature* **508**, 550-553
- 641 13. Costa, T. R., Ilangovan, A., Ukleja, M., Redzej, A., Santini, J. M., Smith, T. K.,
642 Egelman, E. H., and Waksman, G. (2016) Structure of the Bacterial Sex F
643 Pilus Reveals an Assembly of a Stoichiometric Protein-Phospholipid
644 Complex. *Cell* **166**, 1436-1444 e1410
- 645 14. Ou, J. T., and Anderson, T. F. (1970) Role of pili in bacterial conjugation.
646 *Journal of bacteriology* **102**, 648-654
- 647 15. Redzej, A., Ukleja, M., Connery, S., Trokter, M., Felisberto-Rodrigues, C.,
648 Cryar, A., Thalassinou, K., Hayward, R. D., Orlova, E. V., and Waksman, G.
649 (2017) Structure of a VirD4 coupling protein bound to a VirB type IV
650 secretion machinery. *The EMBO journal*
- 651 16. Schroder, G., Krause, S., Zechner, E. L., Traxler, B., Yeo, H. J., Lurz, R.,
652 Waksman, G., and Lanka, E. (2002) TraG-like proteins of DNA transfer
653 systems and of the *Helicobacter pylori* type IV secretion system: inner
654 membrane gate for exported substrates? *Journal of bacteriology* **184**,
655 2767-2779
- 656 17. Byrd, D. R., and Matson, S. W. (1997) Nicking by transesterification: the
657 reaction catalysed by a relaxase. *Molecular microbiology* **25**, 1011-1022
- 658 18. Ilangovan, A., Kay, C. W. M., Roier, S., El Mkami, H., Salvadori, E., Zechner,
659 E. L., Zanetti, G., and Waksman, G. (2017) Cryo-EM Structure of a Relaxase
660 Reveals the Molecular Basis of DNA Unwinding during Bacterial
661 Conjugation. *Cell* **169**, 708-721 e712
- 662 19. Bolland, S., Llosa, M., Avila, P., and de la Cruz, F. (1990) General
663 organization of the conjugal transfer genes of the IncW plasmid R388 and
664 interactions between R388 and IncN and IncP plasmids. *Journal of*
665 *bacteriology* **172**, 5795-5802
- 666 20. Llosa, M., Bolland, S., and de la Cruz, F. (1994) Genetic organization of the
667 conjugal DNA processing region of the IncW plasmid R388. *Journal of*
668 *molecular biology* **235**, 448-464
- 669 21. de Paz, H. D., Sangari, F. J., Bolland, S., Garcia-Lobo, J. M., Dehio, C., de la
670 Cruz, F., and Llosa, M. (2005) Functional interactions between type IV
671 secretion systems involved in DNA transfer and virulence. *Microbiology*
672 *(Reading, England)* **151**, 3505-3516
- 673 22. Fernandez-Lopez, R., Garcillan-Barcia, M. P., Revilla, C., Lazaro, M., Vielva,
674 L., and de la Cruz, F. (2006) Dynamics of the IncW genetic backbone imply
675 general trends in conjugative plasmid evolution. *FEMS microbiology*
676 *reviews* **30**, 942-966
- 677 23. Boer, R., Russi, S., Guasch, A., Lucas, M., Blanco, A. G., Perez-Luque, R., Coll,
678 M., and de la Cruz, F. (2006) Unveiling the molecular mechanism of a
679 conjugative relaxase: The structure of TrwC complexed with a 27-mer

- 680 DNA comprising the recognition hairpin and the cleavage site. *Journal of*
681 *molecular biology* **358**, 857-869
- 682 24. Guasch, A., Lucas, M., Moncalian, G., Cabezas, M., Perez-Luque, R., Gomis-
683 Ruth, F. X., de la Cruz, F., and Coll, M. (2003) Recognition and processing
684 of the origin of transfer DNA by conjugative relaxase TrwC. *Nature*
685 *structural biology* **10**, 1002-1010
- 686 25. Grandoso, G., Avila, P., Cayon, A., Hernando, M. A., Llosa, M., and de la Cruz,
687 F. (2000) Two active-site tyrosyl residues of protein TrwC act
688 sequentially at the origin of transfer during plasmid R388 conjugation.
689 *Journal of molecular biology* **295**, 1163-1172
- 690 26. Alperi, A., Larrea, D., Fernandez-Gonzalez, E., Dehio, C., Zechner, E. L., and
691 Llosa, M. (2013) A translocation motif in relaxase TrwC specifically affects
692 recruitment by its conjugative type IV secretion system. *Journal of*
693 *bacteriology* **195**, 4999-5006
- 694 27. Llosa, M., Grandoso, G., Hernando, M. A., and de la Cruz, F. (1996)
695 Functional domains in protein TrwC of plasmid R388: dissected DNA
696 strand transferase and DNA helicase activities reconstitute protein
697 function. *Journal of molecular biology* **264**, 56-67
- 698 28. Chandler, M., de la Cruz, F., Dyda, F., Hickman, A. B., Moncalian, G., and
699 Ton-Hoang, B. (2013) Breaking and joining single-stranded DNA: the HUH
700 endonuclease superfamily. *Nature reviews. Microbiology* **11**, 525-538
- 701 29. Nivaskumar, M., and Francetic, O. (2014) Type II secretion system: a
702 magic beanstalk or a protein escalator. *Biochimica et biophysica acta*
703 **1843**, 1568-1577
- 704 30. Phan, G., Remaut, H., Wang, T., Allen, W. J., Pirker, K. F., Lebedev, A.,
705 Henderson, N. S., Geibel, S., Volkan, E., Yan, J., Kunze, M. B., Pinkner, J. S.,
706 Ford, B., Kay, C. W., Li, H., Hultgren, S. J., Thanassi, D. G., and Waksman, G.
707 (2011) Crystal structure of the FimD usher bound to its cognate FimC-
708 FimH substrate. *Nature* **474**, 49-53
- 709 31. Geibel, S., Procko, E., Hultgren, S. J., Baker, D., and Waksman, G. (2013)
710 Structural and energetic basis of folded-protein transport by the FimD
711 usher. *Nature* **496**, 243-246
- 712 32. Bakkes, P. J., Jenewein, S., Smits, S. H., Holland, I. B., and Schmitt, L. (2010)
713 The rate of folding dictates substrate secretion by the Escherichia coli
714 hemolysin type 1 secretion system. *The Journal of biological chemistry*
715 **285**, 40573-40580
- 716 33. Akeda, Y., and Galan, J. E. (2005) Chaperone release and unfolding of
717 substrates in type III secretion. *Nature* **437**, 911-915
- 718 34. Radics, J., Konigsmair, L., and Marlovits, T. C. (2014) Structure of a
719 pathogenic type 3 secretion system in action. *Nature structural &*
720 *molecular biology* **21**, 82-87
- 721 35. Vergunst, A. C., Jansen, L. E., Fransz, P. F., de Jong, J. H., and Hooykaas, P. J.
722 (2000) Cre/lox-mediated recombination in Arabidopsis: evidence for
723 transmission of a translocation and a deletion event. *Chromosoma* **109**,
724 287-297
- 725 36. Lang, S., Gruber, K., Mihajlovic, S., Arnold, R., Gruber, C. J., Steinlechner, S.,
726 Jehl, M. A., Rattei, T., Frohlich, K. U., and Zechner, E. L. (2010) Molecular
727 recognition determinants for type IV secretion of diverse families of
728 conjugative relaxases. *Molecular microbiology* **78**, 1539-1555

- 729 37. Draper, O., Cesar, C. E., Machon, C., de la Cruz, F., and Llosa, M. (2005) Site-
730 specific recombinase and integrase activities of a conjugative relaxase in
731 recipient cells. *Proceedings of the National Academy of Sciences of the*
732 *United States of America* **102**, 16385-16390
- 733 38. Agundez, L., Machon, C., Cesar, C. E., Rosa-Garrido, M., Delgado, M. D., and
734 Llosa, M. (2011) Nuclear targeting of a bacterial integrase that mediates
735 site-specific recombination between bacterial and human target
736 sequences. *Applied and environmental microbiology* **77**, 201-210
- 737 39. Johnsson, N., and Varshavsky, A. (1994) Ubiquitin-assisted dissection of
738 protein transport across membranes. *The EMBO journal* **13**, 2686-2698
- 739 40. Eroshenko, N., and Church, G. M. (2013) Mutants of Cre recombinase with
740 improved accuracy. *Nature communications* **4**, 2509
- 741 41. Atmakuri, K., Cascales, E., and Christie, P. J. (2004) Energetic components
742 VirD4, VirB11 and VirB4 mediate early DNA transfer reactions required
743 for bacterial type IV secretion. *Molecular microbiology* **54**, 1199-1211
- 744 42. Thomason, L. C., Costantino, N., Shaw, D. V., and Court, D. L. (2007)
745 Multicopy plasmid modification with phage lambda Red recombineering.
746 *Plasmid* **58**, 148-158
- 747 43. Sharan, S. K., Thomason, L. C., Kuznetsov, S. G., and Court, D. L. (2009)
748 Recombineering: a homologous recombination-based method of genetic
749 engineering. *Nature protocols* **4**, 206-223
- 750 44. Warming, S., Costantino, N., Court, D. L., Jenkins, N. A., and Copeland, N. G.
751 (2005) Simple and highly efficient BAC recombineering using galK
752 selection. *Nucleic acids research* **33**, e36
- 753 45. Mosberg, J. A., Lajoie, M. J., and Church, G. M. (2010) Lambda red
754 recombineering in *Escherichia coli* occurs through a fully single-stranded
755 intermediate. *Genetics* **186**, 791-799
- 756 46. Amyot, W. M., DeJesus, D., and Isberg, R. R. (2013). Poison domains block
757 transit of translocated substrates via the *Legionella pneumophila* Icm/Dot
758 system. *Infection and Immunity* **81**, 3239-3252
- 759

Figure 1

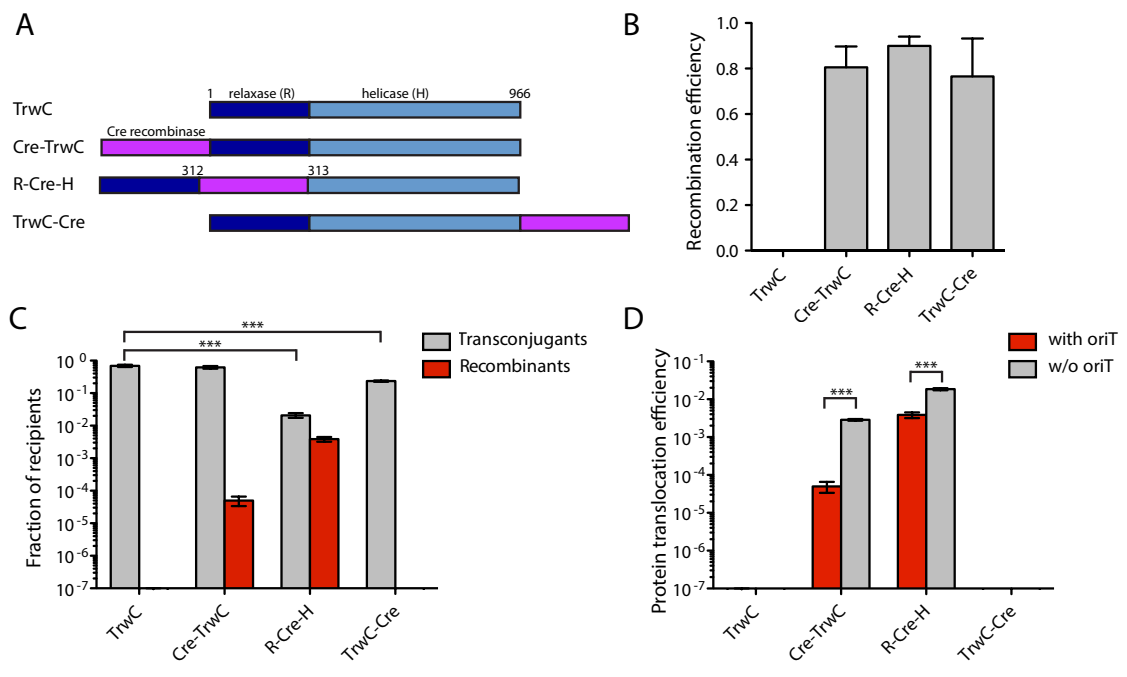


Figure 2

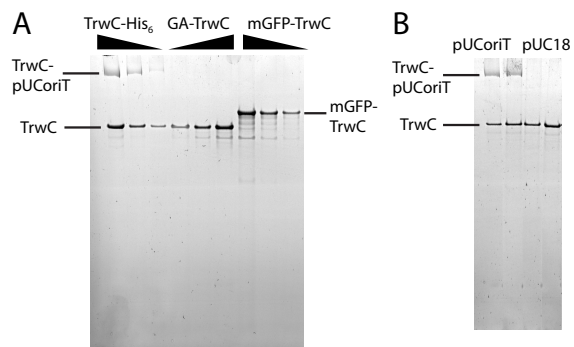


Figure 3

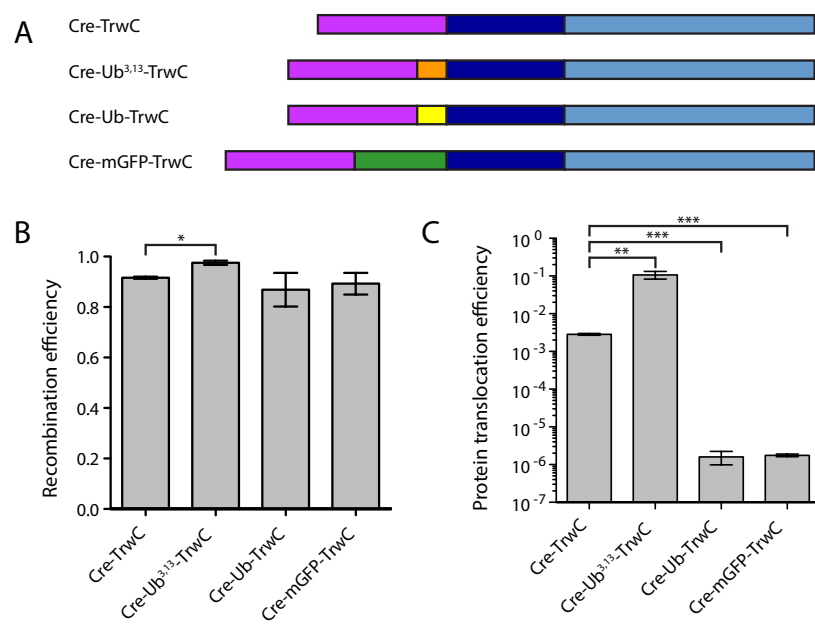
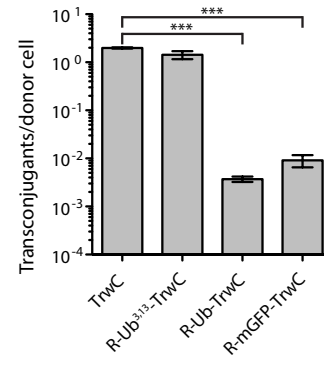
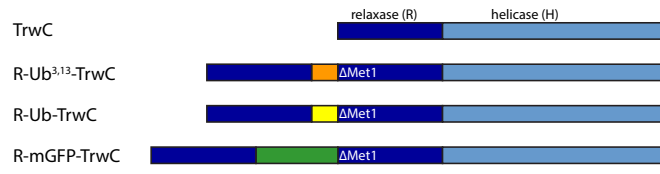
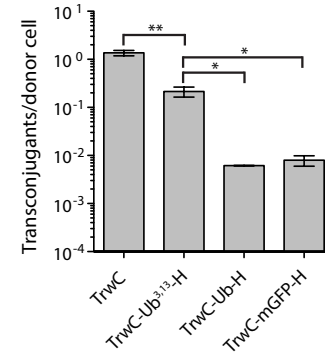
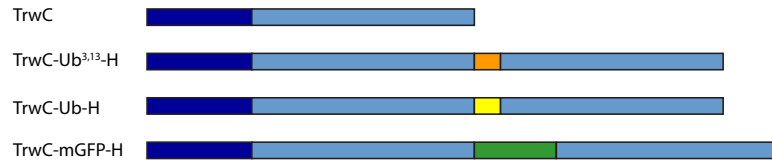


Figure 4

A



B



C

